ISSN 0024-9521
IJG Vol. 42, No. 1, June 2011 (1 - 24)

INDONESIAN JOURNAL OF GEOGRAPHY

ANALYZING RUNOFF DYNAMICS THROUGH PARAMETERIZING A HYDROLOGICAL MODEL IN A WATERSHED: A CASE STUDY IN UPPER SERAYU BASIN, CENTRAL JAVA PROVINCE, INDONESIA

Adhi Nurul Hadi
adhi_akhtar@yahoo.co.id
Natural Resources Conservation Center Aceh, The Ministry of Forestry Republic of Indonesia

Sudibyakto
sudibyakto@gmail.com
Geo-information for Spatial Planning and Risk Management,
Faculty of Geography Gadjah Mada University

Dhruba Shrestha
shrestha@itc.nl
Faculty of Geo-information and Earth Observation, University of Twente
Enschede, The Netherlands

ABSTRACT

This research constructed a hydrological model by means of available data, hydrological equations, and GIS program to find out the runoff dynamic on the study area. The runoff dynamic was analyzed by describing runoff on different land cover types, figuring the correlation between hydrological component and runoff, calculating the sensitivities of the hydrological components to runoff, and identifying the response of runoff to possible land cover change. The model resulted that the highest runoff occurred on built up area and the lowest occurred on cultivation area. Infiltration was also the hydrological component that mostly influenced runoff. Replacing forest, shrub, and plantation by cultivation greatly reduced runoff up to 49 %. Enlarging forest area increased runoff about 12 %. Based on those findings, the hydrological component having the strongest correlation with runoff gave the most influence to runoff change, and enlarging forest area does not always decrease runoff.

Keywords: Flood, hydrological model, runoff, Serayu Hulu, Merawu

INTRODUCTION

In Indonesia, flood is the disaster having the highest frequency comparing to others such as landslide, tsunami, and earthquake. Indonesian National Board for [*Disaster Management,* 2009] showed that floods occurred 198 times, 15 percent of all disasters occurrences, on 2008, and 339 times or 38 percent of all disasters occurrences on 2007. Those two data sets show that floods occurred more often than other disasters and they have caused losses to infrastructures, damage environments and even loss of lives.

Upper area of Serayu watershed, located mostly on Wonosobo district, affects other district located as the next lower, Banjarnegara, in term of flooding hazard. [*Suryanto,* 2010] stated that on May 15, 2010, a flashflood occurred on Susukan, one of sub districts in Banjarnegara and it wiped some settlements located in surrounding Serayu River. At the same time, a flood also inundated other Sub district, Purwareja Klampok, about 10-20 cm. Two factors on the upper area of Serayu Watershed that hypothetically can trigger the occurrences of floods on the lowland areas are natural event and human activities.

The changes of hydrologic cycle on the upper area of Serayu watershed affected the raise of water level on the down river and the changes depend on components of hydrological cycle. Some of factors determining value or level of each component in the hydrological cycle are temperature, humidity, land cover, land use, topography, geomorphology, and soil properties. Those factors can closely represent the character of hydrological cycle in the upper area of Serayu Watershed through constructing a hydrological model by means of hydrology equations, supporting data, and Geographic Information System (GIS). Related to flooding, the constructed hydrological model can represent runoff dynamics on the upper area of Serayu Watershed. The runoff dynamics on the upper area of Serayu watershed can be used as base information in flood analyzing, mitigation, and prediction so an analysis of runoff dynamics through parameterizing a hydrological model in the upper area of Serayu Watershed is required or needed as a support in solving flood problems. The hydrological model furthermore can be used in constructing an early warning system in the Serayu Watershed management.

Study area is located in Serayu which is one of the biggest watersheds in Java Island. It is located between 110^0 4’ 12”E and 109^0 41’ 24”E longitudes and between 7^0 27’ 36”S and 7^0 10’ 48”S latitudes (dotted area on fig.1)

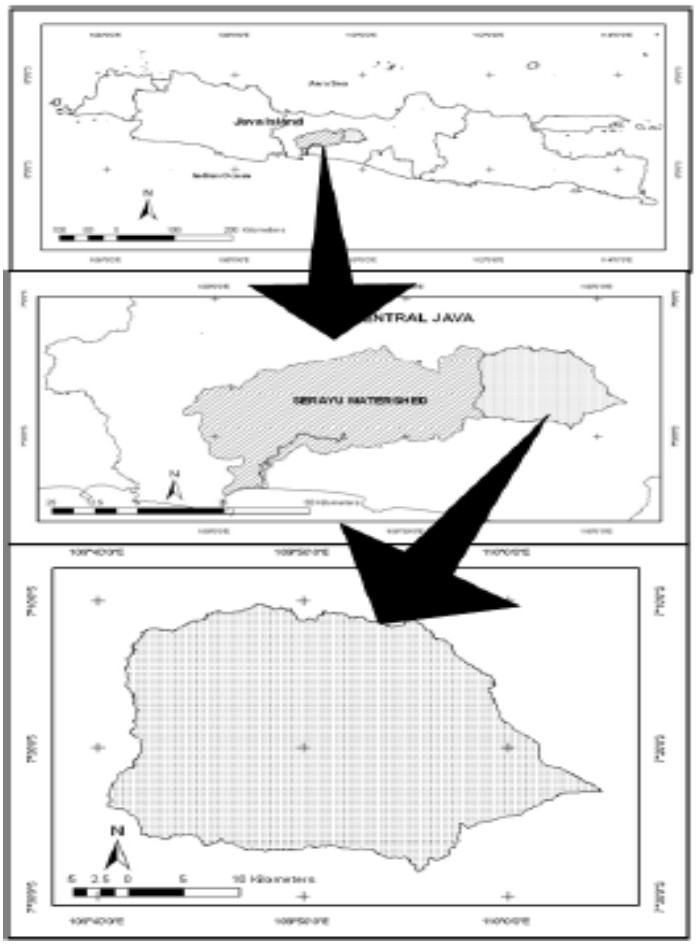

Figure 1. Location of study area

With total area 95,173.65 ha, the study area occupies the upper part of the Serayu Watershed which consists of four Sub Watersheds. They are Serayu Hulu, Begaluh, Tulis, and Merawu Sub Watersheds. There are two stations measuring discharges on the study area. First station is located on 109^0 41' 34.9"E longitudes and 7^o 23' 19.2"S latitudes, and second station is located on 109^0 41' 35.2"E longitudes and 7^o 21' 37.7"S latitudes. First station, Banjarnegara station, located on Banjarnegara bridge, measured discharge coming from Serayu hulu, Begaluh, and Tulis Sub Watersheds. Second station, Clangap station, located on Clangap dam, mesured discharge coming from Merawu Sub Watershed. According to locations of discharge stations, the research divided the study area into two Sub Watersheds. Serayu Hulu, Begaluh, and Tulis Sub Watersheds were considered as one Sub Watershed, Integrated Serayu Hulu Sub Watershed, and Merawu Sub Watershed was still considered as one Sub Watershed. The locations of discharge stations and the Sub Watersheds are shown by fig. 3.

The elevation of study area varies from 237 to 3037 meters above sea level and the climate is characterized by having an equatorial tropical climate with mean annual rainfall varying from 1700 mm up to 4200 mm per year [*Rustanto*, 2010). The area has two main seasons, rainy season and dry season. Rainy season occurs during November to April, while dry season falls during May to October. About 73 percent of mean annual rainfall falls in the rainy season.

Fig. 2 shows monthly rainfall from January 2008 to December 2009. Rainfall data were collected from thirteen rainfall gauges within the study area.

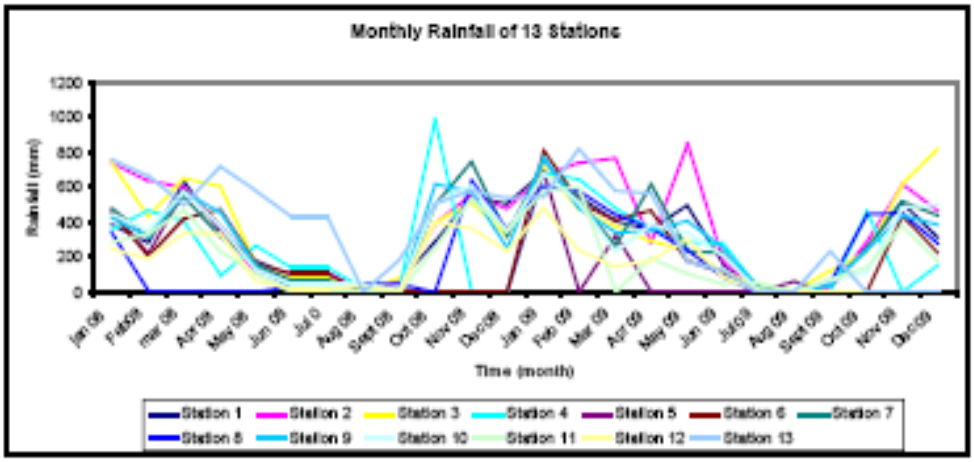

Figure 2. Monthly rainfalls

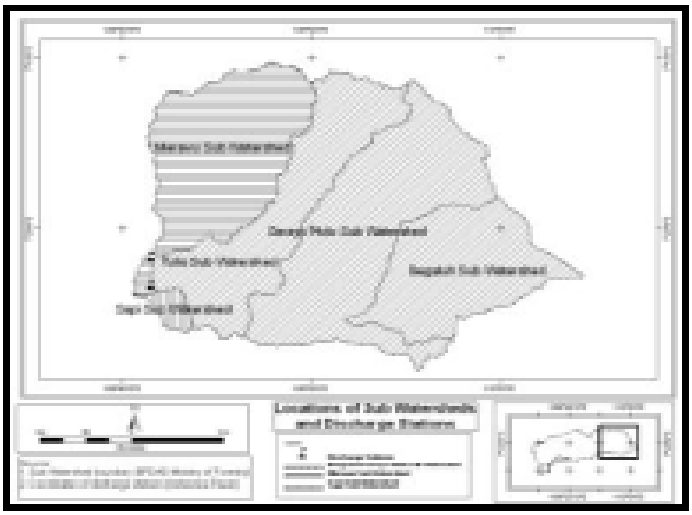

Figure 3. Location of discharge stations and Sub Watersheds

Mean temperature in the area is around 14 up to 27^0 C. At higher elevation and particularly in Dieng plateau the temperature can be cooler with annual mean temperature of 14^0C. Mountains relief with relatively steep slope crosses the northern part of study area (from Wanayasa to Kejajar Sub districts). On the eastern part, there are two high mountains, Sindoro Mountain with height of 3136 meters above sea level and Sumbing Mountain with height of 3340 meters above sea level. The south part is restricted by mountains relief with relatively moderate slope crossing from Banjarnegara to Sapuran Sub districts. The lowest area lies in the southwestern part of the study area (Banjarnegera Sub district).

THE METHODS

Primary data which consisted of daily rainfall from 13 rainfall gauges, hydrographs from two discharge stations, and daily temperature from one station, cumulative infiltration, soil moisture, and soil bulk density were collected from institutions and field observation. MOD13Q1 from June 25, 2008 to Audust 29, 2009 (28 imageries), Digital land cover map of 2009 (at resolution of 30m x 30m), Digital soil texture map (at resolution of 30m x 30m), monthly solar radiation from June 2008 to August 2009 (at resolution of 30m x 30m), Digital Elevation Model (at resolution of 30mx 30m), and river network map (at scale of 1 : 25000), as secondary data, were obtained from literatures, databases and calculation. The research was based on a simple event base hydrological model representing the hydrological processes in the upper part of Serayu Watershed. Runoff Dynamics, as results of the model, were analyzed by observing the hydrological components affecting the runoff dynamics.

Constructing a dynamic hydrological model

The research constructed a dynamic hydrological model, which contains the basic water balance processes, rainfall, interception, evapotranspiration, infiltration, and runoff, and does not take account of base flow aspect. The model was built in daily and starts from July 1, 2008 to August 31, 2009. The research runs all the data in 30 m x 30 m pixel size. NutShell 3.4, a GIS computer program to facilitate the running of PCRaster commands and edit and run PCRaster models, was used to run the model.

Rainfall

Monthly rainfall data and the altitude of rainfall gauges were plotted to scattered graph to figure the relationships between rainfall intensity and altitude. Monthly rainfall data from January to February were plotted to represent East-Asia monsoon condition, and monthly rainfall data from July to September were used to represent Indo-Australian monsoon. Fig. 4 and 5 show the correlation between monthly rainfall and altitude in two monsoon seasons.

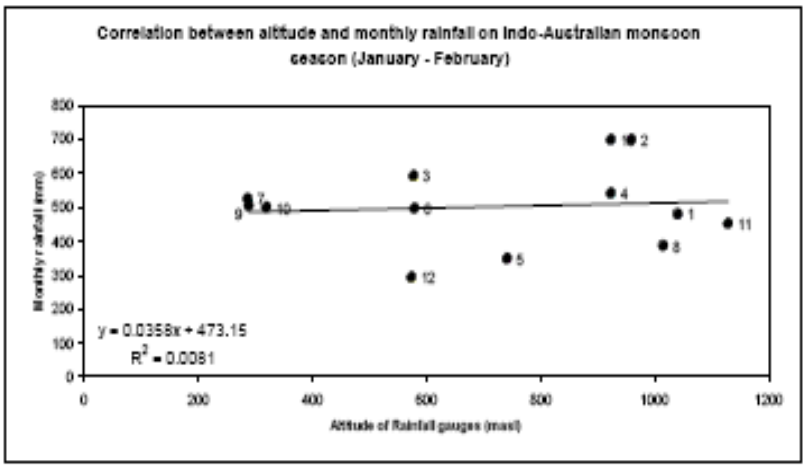

Figure 4. Correlation between altitude and monthly rainfall on Indo-Austrian monsoon

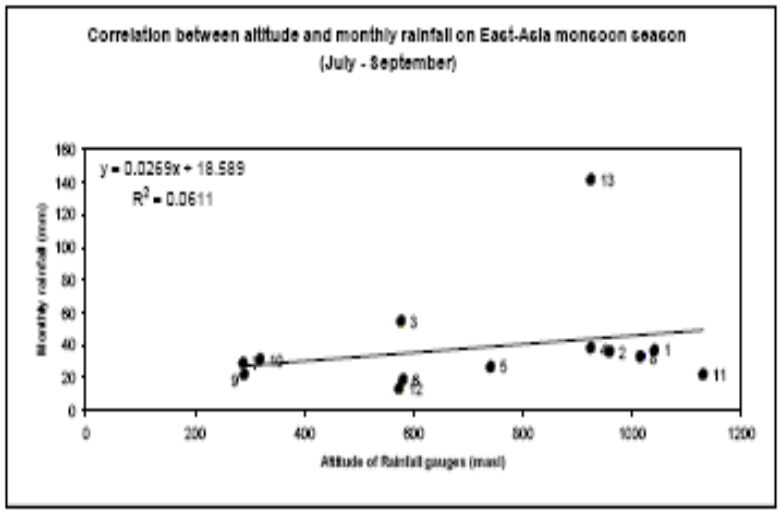

Figure 5. Correlation between altitude and monthly rainfall on East-Asia monsoon

The figures show that correlation coefficient between monthly rainfall and altitude were positive. The square of correlation coefficients resulted from the graphs were very low, $R^2 = 0.0081$ for East-Asia monsoon and $R^2 = 0.0611$ for Indo-Australian monsoon.

The research also plotted all monthly rainfall for the period 2008 – 2009 and altitudes of the gauges into scattered graph. Table 1 shows the square of correlation coefficient between each monthly rainfall and altitude for the period 2008 – 2009.

Table 1 shows that more than half of correlation coefficients between monthly rainfall and altitude in each month were negative (seven of twelve coefficient were negative). Positive coefficients appeared in February, March, May, July, and September, but they were very low, from 0.0057 to 0.2694. Those squares of correlation coefficients were lower than the squares of correlation coefficient calculated by [*Baruti,* 2004], 0.6333, showing that relationship between monthly rainfall and altitude during research period was very weak. Based on those facts, the relationship between altitude and rainfall intensity was not involved in the model.

Table 1. Square of correlation coefficient between each monthly rainfall and altitude for the period 2008 – 2009

Month	Square of Correlation coefficients (R^2)	Correlation coefficient (R)
January	0.05680	-0.2383
February	0.07256	0.2694
March	0.00003	0.0057
April	0.13878	-0.3725
May	0.02078	0.1442
June	0.00265	-0.0515
July	0.06306	0.2511
August	0.05896	-0.2428
September	0.07078	0.2660
October	0.00170	-0.0412
November	0.02588	-0.1609
December	0.01227	-0.1108

Respecting to the dense and distribution of rainfall gauges on the study area (shown by fig.6), which is inappropriate to be used in interpolation method, and weak correlation between rainfall intensity and altitude on the study area during research period, the research decided touse thiessen polygon to determine spatial distribution of rainfall intensity in the model.

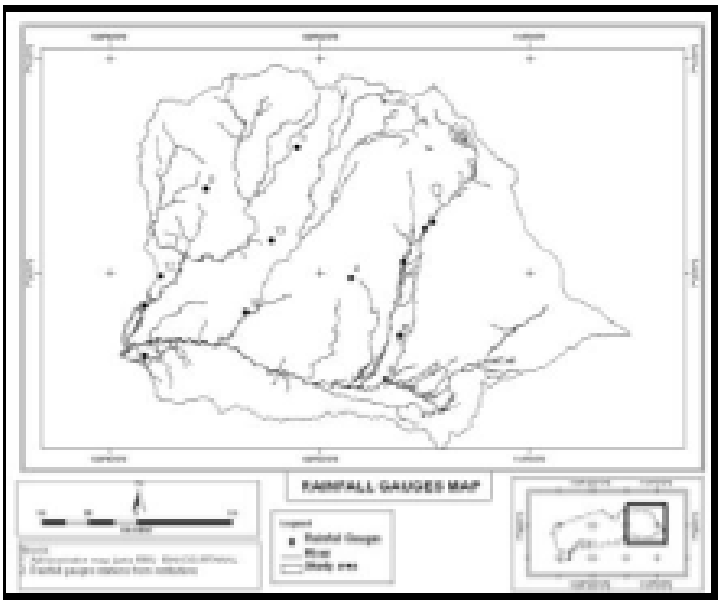

Figure 6. Rainfall gauges map

To get reasonable values of NDVI, the 28 imageries was selected and filtered before they were applied into the model. Selection was carried by visualization in which the imageries generally representing bad form were removed from data lists. Imageries filtering were done in two steps. First step was removing anomalous pixel values suspected as clouds and its shadow by applying a threshold value. Second step was eliminating the pixels having NDVI values suddenly

dropped or increased and then returned to near the previous NDVI values. This eliminating method has been used by [*Xiaoxia, Jixian et al.,* 2008], as Best Index Slope Extraction (BISE), to remove clouds population in NDVI imageries. The equations used in the eliminating process are:

$$dNDVI_{t-1,t} = \frac{(NDVI_{t-1} - NDVI_t)}{NDVI_{t-1}} * 100\% \quad \text{.....(3.1)}$$

$$dNDVI_{t+1,t} = \frac{(NDVI_{t+1} - NDVI_t)}{NDVI_{t+1}} * 100\% \quad \text{.....(3.2)}$$

where $NDVI_{t-1}$ and $NDVI_{t+1}$ denote the NDVI values of time t-1 and t+1 respectively; $dNDVI_{t-1,t}$ and $dNDVI_{t,t+1}$ show the variation rate from t-1 to t and from t+1 to t respectively. It is assumed that the pixel at time t is affected by clouds if $dNDVI_{t-1,t}$ and $dNDVI_{t,t+1}$ are both surpass 20%, then the t time pixel value is corrected by the average of time t-1 and time t+1 [*Xiaoxia, Jixian et al.*, 2008].

This research assumed that the pixel at time t is affected by clouds if dNDVIt-1, and dNDVIt,t+1 are both surpass 30%, 10% higher than value used by [*Xiaoxia, Jixian et al.,* 2008] because the types of vegetation on the study area possibly could reach that percentage (30%) at least at MODIS time range (16 days). On the other hand, the condition of weather on the study area also supports that change of NDVI value.

The research used an equation developed by Campbell and Norman in Kuriakose (2006) to obtain Leaf Area Index (LAI) from NDVI,. The equation is:

$$LAI = -2\ln(1-fc) \quad \text{.....(3.3)}$$

Where, fc is the fractional vegetation cover.
Fractional vegetation cover was determined by using equation suggested by Walthall et. al. in [*Kuriakose,* 2006]. The equation is as follow:

$$Fc = \left[\frac{NDVImax - NDVi}{NDVImax - NDVI\,min} \right] \quad kc \quad \text{.....(3.4)}$$

Where, NDVI max is the maximum NDVI for each used imagery, NDVImin is the minimum NDVI for each used imagery, NDVIi is the NDVI of a particular cell, and kc is the crop factor of the respective land use. The research used crop factor provided by [*Allen, Pereira et al.,* 1998] as FAO Irrigation and Drainage Paper 56.

Maximum storage capacity of canopy was assumed as interception capacity and it was calculated by applying the equation proposed by Von Hoyningen-Huene in [*De Jong and Jetten*, 2007; *Bulcock and Jewitt,* 2010]. The equation is:

$$Smax = 0.935 + 0.498(LAI) - 0.00575(LAI2) \quad \text{.....(3.5)}$$

The storage Smax was filling up with rainfall and emptying with evaporation, and interception could not become more than Smax.

Evapotranspiration

According to collected available data, the research selected Hargreaves equation in [*Yates and Strzepek,* 1994] to determine evapotranspiration in the model. The equation is:

$$Erc = 0.0022*RA*\,'T0.5*(T+17.8) \quad \text{.....(3.6)}$$

Where:

E_{rc} = reference evapotranspiration (mm/day) = Potential evapotranspiration

R_A = mean extra-terrestrial radiation (mm/day)

δ'_T = mean monthly maximum temperature – mean monthly minimum temperature for the month of interest (^oC)

T = mean air temperature (^oC)

Mean extra-terrestrial radiation was calculated by using point solar radiation, an extension provided by Arcgis 9.2, and Temperature was obtained from one temperature station located on 9165983 E longitudes and 369749 S latitudes at 292 masl.

Actual evapotranspiration equal to actual transpiration plus actual evaporation and was determined by following equations.

Ta = Erc*fc*Kc(3.7) Ea = Erc*(1-Kc) ……(3.8)
ETa = TA+Ea ……......(3.9)

Where:
Eta = actual evapotranspiration (mm)
Erc = potential evapotranspiration (Etp) (mm)
fc = fractional vegetation cover
Kc = Crop factor

Infiltration

The research determined daily infiltration by calculating soil moisture storage capacity, Rc. The storage capacity was calculated by following equation.

RC = MS*BD*EHD*(Eta/ET0) ……(3.10)

Where:
RC = Soil Moisture Storage Capacity (mm)
MS = soil moisture content at field capacity (%) BD= Bulk density (mg/m3)
EHD = Effective Hydrological Depth (mm)
Eta/ET0 = Ratio of actual to potential evapotranspiration [*Baruti,* 2004; *Rustanto,* 2010]

Other researcher, [*Basayigit and Dinc*, 2010], added a power, 0.5, to the ratio of actual to potential evapotranspiration, then the equation became:

RC = 1000MS*BD*EHD*(Eta/ET0)0.5 ……(3.11)

This research used the second equation, provided by [*Basayigit and Dinc,* 2010].

Runoff

This research determined runoff value in the model using the equation as follow:

Runoff =rainfall – (potential evapotranspiration + interception + Infiltration)..(3.12)

In the model, runoff was applied by using LDD (Local Drain Direction), one of functions in the nutshell that creates a map representing direction of flow of water from each cell to its steepest down slope neighbor. LDD links each cell and creates a line network as flow pattern. The model is described by the flowing chart (fig.7).

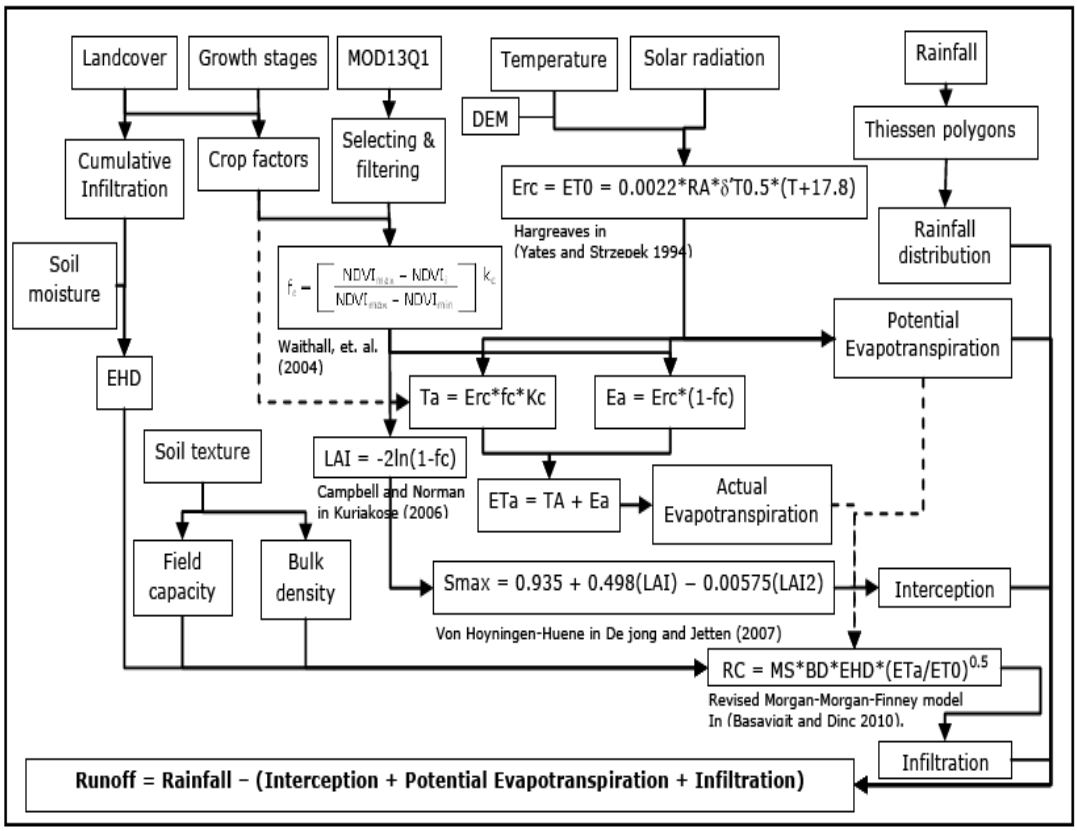

Figure7. A flowchart describing model construction

Analyzing runoff dynamics

Comparing modeled and measured runoffs

Modeled runoff was produced by the model and measured runoff was obtained from the hydrographs by purposing Fixed time method [*Wanielista, Kersten et al.* 1997] assuming that surface runoff always ends after a fixed time interval. The fixed time interval was determined by equation as follow.

$\tau = (DA)n$ ……...(3.13)

Where:
τ = Time from the peak to the end of the runoff hydrograph (days)
DA = Drainage area (miles2)
N = recession constant (0.2)

Modeled runoff was compared to measured runoff in monthly unit by involving Pearson Product Moment Correlation method [*McCuen,* 1998]. The method applies the following equation to determine the correlation coefficient between variables.

$$R = \frac{\Sigma_{xiyi} - ((\Sigma_{xi}\Sigma_{xi}) / n)}{(\Sigma_{xi}^2 - ((\Sigma_{xi})^2 / n))^{0,5} . (\Sigma_{yi}^2 - ((\Sigma_{yi})^2 / n))^{0.5}} \quad \ldots\ldots\ldots\ldots\ldots\ldots\ldots\ldots (3.14)$$

Where:
R = Correlation coefficient yi = Value of variable y
xi = Value of variable x

3.2.2. Identifying the correlation between each hydrological component and modeled runoff

The correlation between each hydrological component, interception, evapotranspiration, or infiltration, and total modeled runoff of two Sub Watersheds was calculated by Pearson Product Moment Correlation method as was done in comparing modeled and measured runoffs.

Evaluating the sensitivity of hydrological components to modeled runoff

In order to determine sensitivities of hydrological components to modeled runoff, the research applied six simulations into the model to run the modified hydrological components. The simulations were:

1. Interception was multiplied by one and half, and other components were remain
2. Interception was multiplied by two, and other components were remain
3. Potential evapotranspiration was multiplied by one and half, and other components were remain
4. Potential evapotranspiration was multiplied by two, and other components were remain
5. Infiltration was multiplied by one and half, and other components were remain
6. Infiltration was multiplied by two, and other components were remain

Analyzing the responses of runoff to possible modified land cover

The research applied three scenarios into the model to identify the responses of runoff to the land cover change. The scenarios were:

1. Replacing cultivation, shrub, and plantation land cover types by forest
2. Replacing cultivation, shrub, and forest land cover types by plantation
3. Replacing plantation, shrub, and forest land cover types by cultivation

RESULT AND DISCUSSION

Characteristics of hydrological components on each land cover type

Total of hydrological components in each land cover type during research period as the result of the model are represented by table 1

Table 1. Total of hydrological component in each land cover type

No	Land cover type	Cumulative interception (mm)	Cumulative potential evapotranspiration (mm)	Cumulative actual evapotranspiration (mm)	Cumulative infiltration (mm)	Cumulative runoff (m3)
1	Built up area	295	734	734 (100 %)	474	1980
2	Paddy field	300	790	819 (104 %)	1257	1074
3	Dry land	352	632	521 (82 %)	2622	74
4	Forest	421	537	496 (92 %)	2535	416
5	Shrub	427	546	442 (81 %)	2817	138
6	Plantation	432	609	509 (83 %)	2735	178
7	Grass land	483	336	278 (83 %)	2487	960

Source: calculated by the model

The highest cumulative interception on the study area during research period was on grassland and the lowest was on built up area. That condition was supported by vegetations growth on those two areas, vegetations on built up area was lower than vegetations on grassland.

The cumulative evapotranspirations on the study area during research period occurred on paddy field and the lowest occurred on Grassland. The difference between potential and actual evapotranspiration is assumed as crop water need [*Pidwirny and Jones,* 2009]. The percentage of actual evapotranspiration to potential evapotranspiration was an implication of crop factors used in the model and represents quantity of water that is actually removed from a surface due to the processes of evaporation and transpiration [*Pidwirny and Jones,* 2009]. The research assumed that on the built up area, all the potential evapotranspiration would became actual evapotranspiration (high actual evapotranspiration) respecting the condition of built up area covered by buildings, asphalt, concrete, and other constructions and inflicting crop water need on the built up area became almost zero. This condition is in line with [*Lin, Velde et al.,* 2008] stating that mixed effect of construction, water body, street trees and grass parcels that have very high evapotranspiration drive the urban areas to have high actual evapotranspiration.

Forest area had relatively high actual evapotranspiration comparing to its potential evapotranspiration, respecting to the condition of forest that generally was still dense. Actual evapotransipration of paddy field was higher than its potential evapotranspiration because this research assumed that almost all the crop factors in paddy filed growth stages were more than one representing irrigation involvement.

The highest infiltration on the study area during research period occurred in Shrub area (2864 mm) and the lowest occurred in the built up area (499mm). Dry land cultivation, forest, shrub, plantation, and grassland had relatively high infiltration (2400 mm – 2900 mm). On the other hand, built up area had the lowest infiltration which was caused by constructions dominantly covered the area, and paddy field also had relatively low infiltration representing the effect of growth stages (stages 1 and 2) in which the area were inundated resulting low infiltration.

Land cover type, which had the highest runoff, was the built up area, with cumulative runoff equaled to 1980 m^3. That fact represents the condition of surface on the built up area which was mostly covered by buildings, asphalt, concrete, and other constructions. Constructions covering surface reduce infiltration capability and increase runoff. The lowest runoff occurred on dry land cultivation. This condition was caused by high effective hydrological depth (EHD) had by dry land cultivation. Effective hydrological depth of dry land cultivation, especially in initial and crop development growth stages, was very high. That EHD could increase soil moisture storage capacity and reduce runoff. In initial growth stage, farmers cultivated the land and made the water on the land infiltrated easily.

Comparing Modeled Runoff and Measured Runoff

Monthly Modeled runoffs of Integrated Serayu Hulu and Merawu Sub Watersheds compared to monthly measured runoffs are shown by graph 8 and 9. According to those graphs, in terms of total runoff, modeled runoff was closer to measured runoff on Integrated Serayu Hulu Sub Watershed than modeled runoff to measured runoff in Merawu Sub Watershed (shown by the position of black fine lines respecting to blue fine lines). In terms of runoff distribution in each month, modeled runoff was closer to measured runoff on Merawu Sub Watershed than modeled runoff to measured runoff in Integrated Serayu Hulu Sub Watershed (shown by the trends of dashed blue lines and dashed black lines).

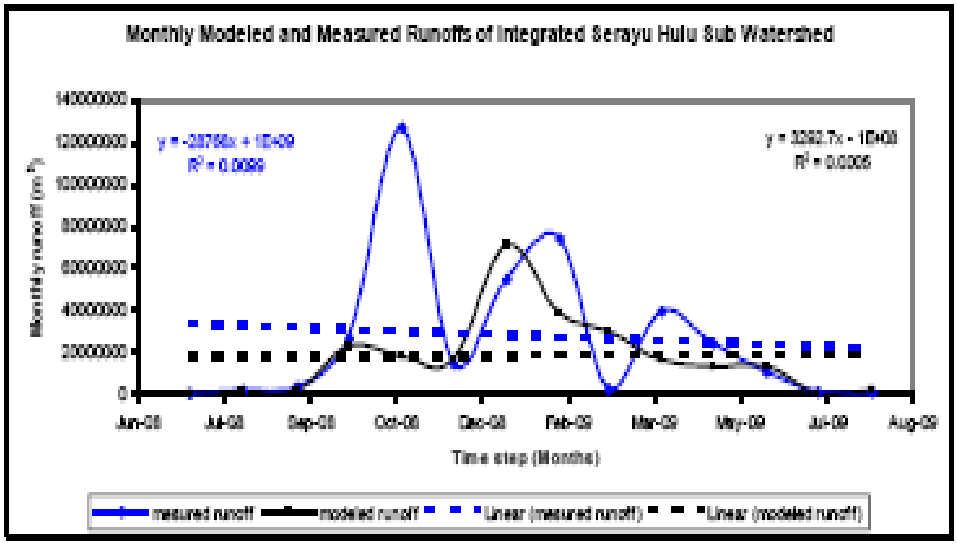

Figure 8. Monthly modeled and measured runoff of in targeted Serayu Hulu sub water shed

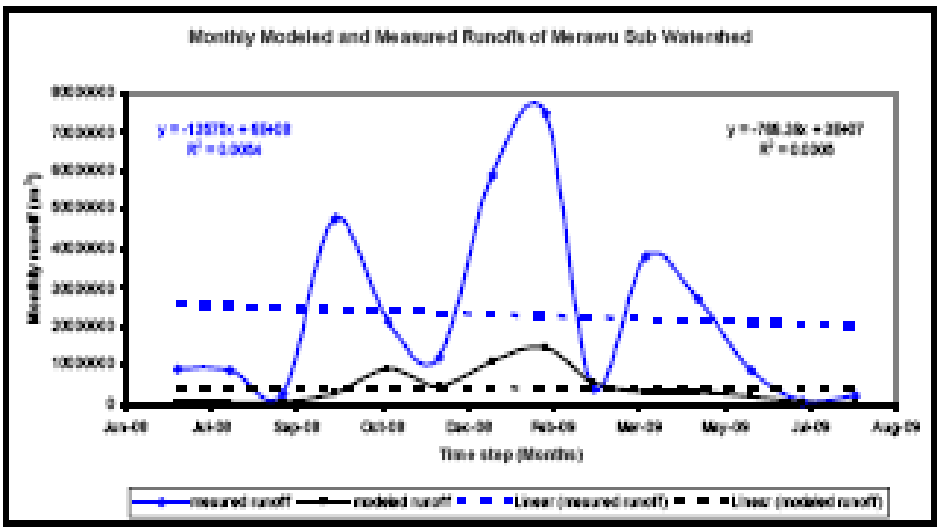

Figure 9. Monthly modeled and measured runoff of Merawu sub water shed

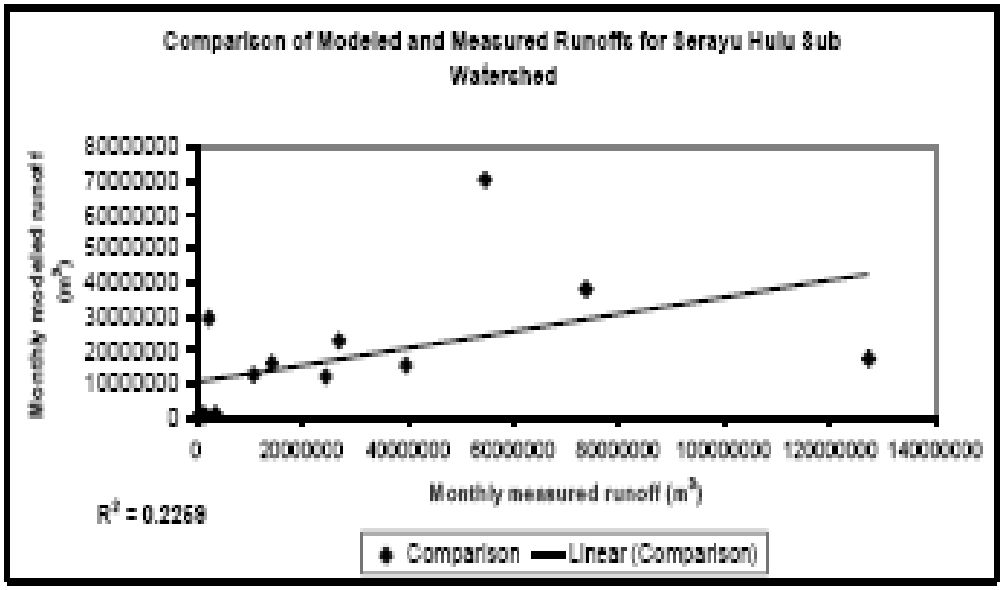

Figure 10. Comparison of modeled and measured runoff on Integrated Serayu Hulu Sub Watershed

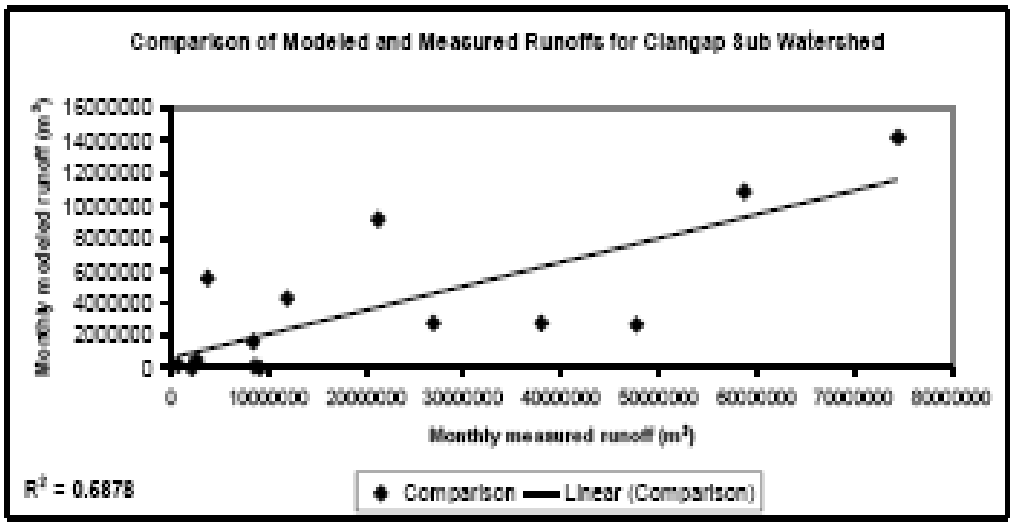

Figure 11. Comparison of modeled and measured runoff on Merawu Sub Watershed

The correlation coefficients, on the Figure 10 and 11 describe the closeness of modeled runoff to measured runoff with assumption that if correlation coefficient equals to one then modeled runoff is exactly same with measured runoff. The graphs show that in Integrated Serayu Hulu Sub Watershed, 22.59% of

the variance in measured runoff could be explained by variance of modeled runoff, and in Merawu Sub Watershed, 58.78 % of the variance in measured runoff could be explained by variance of modeled runoff.

Table 2 shows the total model runoffs on two Sub Watersheds during research period compared to total measured runoffs from two discharge stations.

Table 2. Modeled runoff compared to measured runoff

No	Sub Watersheds	Total runoffs during 14 months	
		Modeled runoff (m^3)	Measured runoff (m^3)
1	Integrated Serayu Hulu	267118807	380333747
2	Merawu	62371385	314490165

According to table 2, the model resulted runoff that were lower than measured runoff, 70.23 % for Integrated Serayu Hulu Sub Watershed, and 19.83 % for Merawu Sub Watershed. Those differences, between modeled and measured runoffs, were caused by deficiencies involved in the research. First, the distribution of rainfall gauges did not fully cover the distribution of rainfall intensity occurring on the study area. Small number and locations of available rainfall gauges on the study area caused this problem. Second, the distribution of samples, 73 cumulative infiltration and bulk density measurements, on the study area was still not proportional to the distribution of land cover on the study area caused by accessibility limitation. Third, growth stages of paddy field and dry land cultivation involved in the model still could not represent the real planting cycle applied by farmers on the study area. The research assumed that all paddy field and dry land cultivation started planting in the same time or each of them has a uniform growth stage. In fact, paddy field and dry land cultivation on the different locations have different growth stages.

This deficiency was caused by limitation in applying various growth stages of a land cover type into model. Fourth, one of soil properties, porosity, involved in the model was obtained from reference, which probably was not appropriate with the condition on the study area.

Correlation between Each Hydrological Component and Modeled Runoff

Total daily runoff, average daily interception, potential evapotranspiration, and infiltration on the study area had been involved in Pearson Product Moment Correlation method to calculate the correlation between each of hydrological component an nd modeled runoff. Results of calculation are shown by table 4.3.

Table 3. Correlation coefficient between hydrological component and modeled runoff

No	Hydrological components	Correlation coefficient between hydrological component and total modeled runoff (R2)
1	Interception	0.3553
2	Potential Evapotranspiration	0.2585
3	Infiltration	0.6638

Source: Calculations carried in Microsoft Office Excel 2003

Table 3 shows that the highest square of correlation coefficient was had by Infiltration-total modeled runoff linear relationship and the lowest one had by potential evapotranspiration-total modeled runoff linear relationship.

Based on table 3, it can be stated that 66.38 % of the variance in the total modeled runoff could be explained by variance of infiltration, 35.53 % of the variance in the total modeled runoff could be explained by variance of interception, and 25.85 % of the variance in the total modeled runoff could be explained by variance of potential evapotranspiration.

Correlation coefficients only determine the strength of linear relationships between each hydrological component and total modeled runoff. They do not represent the level of causality or effect between hydrological component and total modeled runoff. Correlation coefficient strongly depends on data distribution of variables involved in linear relationship. Correlation coefficient does not describe the causality between variables but it shows the responses of variables to factor that mainly affected their values or levels. In this research, the factor mostly affecting values or levels of hydrological components was rainfall.

Sensitivities of Hydrological Components to Modeled Runoff

Table 4 shows the results of the processes representing the changes of hydrological component values and their effects to modeled runoff. Based on table 4, the most sensitive component to runoff in the model was infiltration. Runoff was raised more than 20 percent when infiltration was increased a half of original value and it raised more than 30 percent when infiltration was increased two times of original value on the other hand, interceptttion and potential evapotranspiration had low sensitivities respecting to infiltration. Runoff decreased about 3.70 – 5.01 percent when interception was added by a half of original value and reduction increased to 8.71 – 11.37 percent when interception was increased two times of original value. Evapotranspiration had relatively same sensitivity with interception. Runoff decreased 5.65 – 6.53 percent when potential evapotranspiration was increased a half of original value and it decreased 11.43 – 13.28 percent when potential evapotranspiration increased two times.

Table 4. The changes of hydrological component values and their effects to runoff

No	Hydrological component changes	Original runoff (m3)		Generated runoff (m3)		Percentage	
		Integrated Serayu HuluSub Watershed	Merawu Sub Watershed	Integrated Serayu Hulu Sub Watershed	Merawu Sub Watershed	Integrated Serayu HuluSub Watershed	Merawu Sub Watershed
1	Interception multiplied by	267118807	62371385	257236264	59245374	-3.70	-5.01
2	Interception multiplied by two	267118807	62371385	243845969	55279166	-8.71	-11.37
3	Potential evapotranspiration multiplied by one and half	267118807	62371385	252026111	58299038	-5.65	-6.53
4	Potential evapotranspiration multiplied by two	267118807	62371385	236574503	54089005	-11.43	-13.28
5	Infiltration multiplied by one and half	267118807	62371385	204971070	46758232	-23.27	-25.03
6	Infiltration multiplied by two	267118807	62371385	178892923	39927885	-33.03	-35.98

Responses of Modeled Runoff to Possible Modified Land cover

Land cover modifications, the scenarios, were applied by reconstructing and rerunning the model. The results of the rerunning model are shown by table 5. Results of scenarios shows that all modifying land covers types, forest, plantation, and cultivation, gave different affect to modeled runoff. Cultivation had the most negative influence to runoff comparing to two other land cover types. It greatly reduced runoff, 35.46 % for Integrated Serayu Hulu Sub Watershed, and 49.92 % for Merawu Sub Watershed. Replacing cultivation, shrub, and plantation by forest, increased modeled runoff on those Sub Watersheds, 12.40 % for Integrated Serayu Hulu Sub Watershed, and 12.25 % for Merawu Sub Watershed.

Table 5. Total modeled runoff as the results of scenarios

No	Scenarios	Original runoff (m3)		Generated runoff (m3)		Percentage	
		Integrated Serayu Hulu Sub Watershed	Merawu Sub I Watershed	Integrated Serayu Hulu Sub Watershed	Merawu Sub Watershed	Integrated Serayu Hulu Sub Watershed	Merawu Sub Watershed
1	Replacing cultivation, shrub, and plantation by forest	267118807.9	62371385.52	300245523.2	70012123.19	12.40	12.25
2	Replacing cultivation, shrub, and forest by	267118807.9	62371385.52	311145170.5	47072327.81	16.48	-24.53
3	Replacing plantation, shrub, and forest by cultivation	267118807.9	62371385.52	172390270.3	31237501.19	-35.46	-49.92

On the other hand, replacing cultivation, shrub, and forest by plantation, increased modeled runoff on Integrated Serayu Hulu Sub Watershed about 16.48 %, meanwhile it decreased modeled runoff on Merawu Sub Watershed about 24.53 %.

Replacing land cover types by cultivation decreased modeled runoff on both Sub Watersheds because combination of cultivation with any soil textures had the highest effective hydrological depth compared to combinations of other land cover types with soil textures. Scenario 1 increased runoffs on both Sub Watersheds because forest that has the lowest infiltration and potential evapotranspiration among the modified land cover types (table 1) replaced the land cover types which had relatively high infiltration. On the other hand, cultivation, shrub, and plantation had larger areas than forest area (table 6) so that condition reduced infiltration capacity and increased runoff on the study area.

Scenario 2, replacing cultivation, shrub, and forest by plantation, decreased modeled runoff on Merawu Sub Watershed because plantation had relatively high interception and infiltration (table 1). Even though plantation had high interception and infiltration, modeled runoff on Integrated Serayu Hulu Sub Watershed was increased by scenario 2. This condition was affected by the difference of soil texture distributions on both Sub Watersheds. Combination of plantation and clay loam had the highest effective hydrological depth in plantation-soil texture combinations and clay loam in Merawu Sub Watershed had larger area (28.77 %)

than clay loam in Integrated Serayu Hulu Watershed (2.22 %), which made the combination, gave more effect in Merawu Sub Watershed than in Integrated Serayu Hulu Sub Watershed. Table 7 shows soil texture distribution in both Sub Watersheds.

Another factor, making scenario two increased modeled runoff on Integrated Serayu Hulu Sub Watershed, was the difference of areas that were replaced by plantation. In scenario two, 52.36 % of Integrated Serayu Hulu Sub Watershed area and 55.71 % of Merawu Sub Watershed area were replaced by plantation. The more areas that were replaced the more effect that was given by plantation, the hydrological component which could greatly raise interception.

Table 6. Areas of land cover types in two Sub Waters heeds

No	Land cover types	Integrated Serayu Hulu Sub Watershed (pixel number)	%	Merawu Sub Watershed (pixel number)	%
1	Built up area	40809	5.35	9281	3.68
2	Paddy field	49666	6.52	7612	3.02
3	Water body	1482	0.19	208	0.08
4	Dry cultivation	173126	22.71	54428	21.58
5	Forest	74920	9.83	37369	14.82
6	Shrub	151012	19.81	48717	19.31
7	Plantation	268289	35.20	94331	37.40
8	Grass land	2862	0.37	279	0.11

Source: Digital land cover map and calculation carried in Arcgis 9.2

Table 7. Areas of soil textures in two Sub Waters heeds

No	Soil texture	Integrated Serayu Hulu Sub Watershed (pixel number)	%	Merawu Sub Watershed (pixel number)	%
1	Clay	98607	12.93	14967	5.93
2	Clay loam	16935	2.22	72602	28.77
3	Loam	175643	23.04	61696	24.45
4	Loamy sand	52344	6.86	-	0
5	Sandy loam	347395	45.56	83879	33.24
6	Silt loam	56991	7.47	-	0
7	Silty clay	14561	1.91	19169	7.60

Source: digital texture map and calculation carried in Arcgis 9.2

CONCLUSIONS

The highest runoff occurred on built up area and the lowest runoff occurred on dry land cultivation. Surface condition and effective hydrological depth of land cover types determined level of runoff on each land cover type.

Modeled runoff on merawu Sub Watershed was closer to measured runoff than modeled runoff on Integrated Serayu Hulu Sub Watershed to measured runoff, and both modeled runoffs on Integrated Serayu Hulu and Merawu Sub Watersheds were lower than measured runoffs on those Sub Watersheds.

Not all hydrological components had negative correlation with total modeled runoff, and the hydrological component, which had the strongest correlation with total modeled runoff, was infiltration.

The hydrological component, which mostly influenced modeled runoff, was infiltration and it can be concluded that the hydrological component having the strongest correlation with runoff gave the most influence to the runoff change. The results of applying scenarios into model show that enlarging forest area does not always decrease runoff. Soil properties also have great effect to the runoff dynamic.

RECOMMENDATIONS

To get more accurately result, more dense sampling points are needed to represent infiltration and soil properties more detail on the study area. Omparing hydrological components and factors affecting the components on two Sub Watersheds, Integrated Serayu Hulu and Merawu, in more detail are required to observe the characteristics of those Sub Watersheds and their affects to runoff on the down stream.

Reconstructing the model using images that have higher or lower accuracy is required to investigate the effect of data accuracy used in the model to the results comparing to the real condition. This can be used to determine accuracy of precise data that can produce result closest to reality. installing equipments in well-distributed position to measure the factors affecting hydrological components, such as wind speed, temperature, humidity, solar radiation, and rainfall intensity is needed to obtain the more accurate and representative data.

ACKNOWLEDGEMENT

I would give my grateful thanks to the Indonesian and Dutch Governments for giving me opportunity to study at Double Degree M.Sc. Programme, Gadjah Mada University, Yogyakarta, Indonesia and Faculty of Geo-Information and Earth Observation, University of Twente, Enschede, The Netherlands.

Many thanks to Gadjah Mada University, Faculty of Geo-Information and Earth Observation-University of Twente, Pusbindiklatren-BAPPENAS, Netherlands Education Support Office, and Ministry of Forestry for their great support during my study.

REFERENCES

Allen, R. G., L. S and Pereira, et al. (1998), *Crop evapotranspiration - Guidelines for computing crop water requirements - FAO Irrigation and drainage paper 56*. Rome, Food and Agriculture Organization of the United Nations.

Baruti, J. H. M. (2004), *Study of Soil Moisture in Relation to Soil Erosion in the Proposed Tancitaro Geopark, Central Mexico, a Case of the Zacandaro sub-watershed*. Department of Earth Systems Analysis Enschede, the International Institute for Geo-information Science and Earth Observation. Master of Science: 92.

Basayigit, L. and U. Dinc (2010), *Of Soil Loss in Lake Watershed Using GIS : A Case Study of Egirdir Lake, Turkey*. Natural & Environmental Sciences 1(1): 1-11.

De jong, S. M. and V. G. Jetten (2007), *Estimating spatial patterns of rainfall interception from remotely sensed vegetation indices and spectral mixture analysis.* International Journal of Geographical Information Science 21(5): 529-545.

Indonesian National Board for Disaster Management (2009), *Disaster Statistics.* Retrieved May20, 2010, 2010, from http://bnpb.go.id/website/index.php?-option=comcontent&task=view&id=2100.

Kuriakose, S. L. (2006), *Effect of Vegetation on Debris Flow Initiation - Conceptualization and Parameterization of a Dynamic Model for Debris Flow Initiation in Tikovil River Basin, Kerala, India using PCRaster®.* Department of Earth Systems Analysis Enschede, the International Institute for Geo-information Science and Earth Observation. Master of Science: 121.

Lin, W., R.v.d. and Velde, et. al. (2008), S*atellite Based Regional-Scale Evapotranspiration in the Hebei Plain, Northeastern China.* 2008 Dragon Symposium (Dragon 1 Programmed Final Results 2004 – 2007), Beijing, P.R.China, European Space Agency and National Remote Sensing Center of China.

McCuen (1998), *Hydrologic Analysis and Design*. New Jersey, Prentice-Hall, Inc.: 833.

Pidwirny, M. and S. Jones (2009), *Introduction to the Hydrosphere Actual and Potential Evapotranspiration.* Retrieved January 10, 2011, from http://www.physicalgeography.net/fundamentals/8j.html.

Rustanto, A. (2010), *Soil Erosion Dynamics Due to Land Use / Land Cover Changes, Case Study in Upper Serayu Watershed, Indonesia.* Department of Earth Systems Analysis Enschede, the International Institute for Geo-information Science and Earth Observation. Master of Science: 73.

Suryanto (2010), *Floods hit Banjarnegara.* Retrieved May 21, 2010, from http://perempuan.kompas.com/read/xml/2010/05/15/13305574/-banjarnegara.diterja ng.banjir.

Wanielista, M., R. Kersten, et al. (1997), *Hydrology Water Quantity and Quality Control*. Canada, John Wiley and Sons, Inc.

Xiaoxia, S., Z. and Jixian, et al. (2008), *Vegetation Cover Annual Changes Based On Modis/Terra Ndvi In The Three Gorges Reservoir Area*. The XXIth ISPRS Congress, Beijing, International Society for Photogrammetry and Remote Sensing.

Yates, D. and K. Strzepek (1994), *Potential Evapotranspiration Methods and their Impact on the Assessment of River Basin Runoff under Climate Change*.